ISSN 1990-7931, Russian Journal of Physical Chemistry B, 2009, Vol. 3, No. 3, pp. 333–347. © Pleiades Publishing, Ltd., 2009.
Original Russian Text © S.M. Frolov, V.Ya. Basevich, F.S. Frolov, A.A. Borisov, V.A. Smetanyuk, K.A. Avdeev, A.N. Gots, 2009, published in Khimicheskaya Fizika, 2009, Vol. 28, No. 5, pp. 3–18.

THE XXXII ACADEMIC READINGS ON COSMONAUTICS. MOSCOW, JANUARY, 2008

Correlation between Drop Vaporization and Self-Ignition

S. M. Frolov[a], V. Ya. Basevich[a], F. S. Frolov[a], A. A. Borisov[a], V. A. Smetanyuk[a], K. A. Avdeev[b], and A. N. Gots[c]

[a] *Semenov Institute of Chemical Physics, Russian Academy of Sciences, ul. Kosygina 4, Moscow, Russia*
[b] *Tula State University, Tula, Russia*
[c] *Vladimir State University, Vladimir, Russia*
e-mail: smfrol@chph.ras.ru

Received August 19, 2008

Abstract—A parametric analysis of numerical solutions to problems of vaporization and self-ignition of liquid hydrocarbon drops was performed, and a new criterion determining the conditions of drop self-ignition was suggested. According to this criterion, self-ignition at a given reduced distance from the drop begins when the required reduced gas temperature and equivalence ratio are reached. A new model of heating and vaporization of drops in dense gas suspensions was suggested. The model was verified in multidimensional calculations of self-ignition and combustion of drop clouds. Calculations showed that the model correctly described the phenomenology of local formation and anisotropic propagation of self-ignition waves in suspensions of drops in gases.

DOI: 10.1134/S1990793109030014

INTRODUCTION

Self-ignition of drops in various energy converters working on liquid fuel and in heterogeneous detonation waves has as a rule been simulated with the use of various heuristic criteria, which do not take into account the complex thermal, dynamic, and chemical interaction of phases in dense sprays and gas suspensions. These factors can, however, substantially influence the time and place of self-ignition and the volume of a mixture enveloped in a self-ignition flash. Because self-ignition is one of key processes determining the construction, size, and regime parameters of modern diesel engines, burners, and combustion chambers of aircraft, correct physicomathematical models of this phenomenon applicable in multidimensional gas dynamic calculations are necessary.

The classic model of the self-ignition of a drop of a fuel is based on the Semenov–Frank–Kamenetskii stationary approximation [1, 2]. One of the earliest models with an infinitely fast chemical reaction was suggested by Varshavskii [3]. In [4, 5], this model was extended to finite chemical reaction rates. Subsequently, the problem was analyzed in [6–9]. As in the stationary theory of thermal explosion, the conditions of drop self-ignition are identified with the conditions under which a stationary solution to the problem of drop vaporization accompanied by gas-phase chemical reactions between oxidizer and vapor-phase fuel disappears. The physical meaning of the absence of a stationary solution reduces to the conclusion that heat conductivity processes in the gas phase cannot balance heat release caused by chemical transformations.

The nonstationary theory of drop self-ignition was developed by Merzhanov et al. [10, 11]. The use of the nonstationary theory, in particular, showed that self-ignition began with the formation of a weak maximum in the spatial temperature distribution at a fairly large distance from the surface of the drop. This distribution then rapidly transformed into a profile characteristic of a flame surrounding the drop.

Simple models of the combustion of drops (e.g., see [2, 3, 12–14]) allow us to estimate the lifetime of a drop, flame temperature, the distance between the surface of the drop and flame front, and some other parameters. However, as applied to the problem of drop self-ignition, simple models are ineffective. To solve this problem, we need data on the dynamics of physicochemical processes inside the drop and in its vicinity. Problem statement must therefore be based on nonstationary equations in partial derivatives describing the distributions of thermodynamic parameters, species concentrations, and velocity both inside the drop and in its vicinity.

Let us consider the most important results obtained by solving this problem in [15–20]. In these works, qualitative and quantitative characteristics of self-ignition of paraffin hydrocarbon fuel drops were studied. It was found that, generally, the self-ignition of drops developed in two stages, as in a homogeneous system. First, a cool flame appeared, and then a hot explosion occurred. In some instances, a blue flame could also be observed.

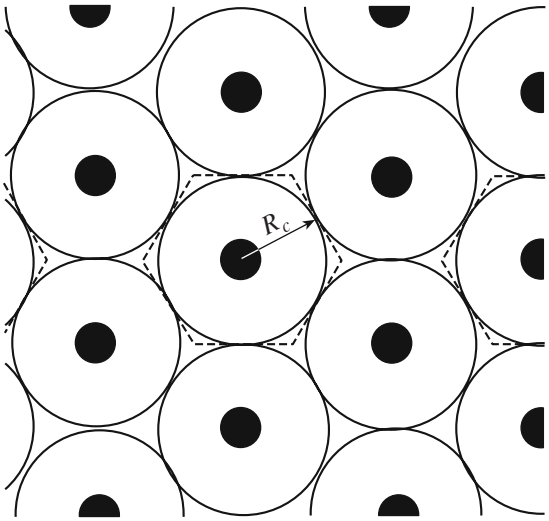

Fig. 1. Definition of an elementary grid cell in a uniform monodisperse gas suspension of drops [19, 20]. Solid circles are drops. Circles around drops characterize the depth of the penetration of diffusion fluxes. The dashed line bounds the elementary cell through the surface of which there are no energy and mass fluxes; R_c is the characteristic size of the cell.

According to [19, 20], small drops have time to vaporize before self-ignition, and cold-flame oxidation occurs in a comparatively large gas volume with almost uniform temperature and concentration fields. For this reason, the cool flame stage is easy to identify using kinetic curves for averaged gas parameters. The conditions of the occurrence of cold-flame oxidation are then close to homogeneous mixture conditions, under which cool flames have been observed experimentally.

Large drops have no time to vaporize before the self-ignition of vapor. In complete correspondence to the classic theory, self-ignition then occurs locally at some distance from the surface of drops, in the region of substantial nonuniformities of temperature and concentration fields. During self-ignition, first the local accumulation of alkylhydroperoxide occurs. This is followed by alkylhydroperoxide decomposition resulting in the appearance of a cool flame, that is, a local increase in the concentration of hydroxyl. With some delay, the cool flame stage is followed by hot explosion, also local. Because of the local character of self-ignition, the cool flame stage is difficult to identify using kinetic curves for averaged gas parameters.

The results of numerical calculations taking into account a detailed or simplified kinetics of chemical transformations as a rule closely agree with the experimentally measured delay times of drop self-ignition. As concerns experimental works on the vaporization and self-ignition of hydrocarbon fuel drops, their number is exceedingly large. Very many publications concerned with this problem can be found in Proceedings of the Annual Congress of the Society of Automotive Engineers (SAE). We shall note only several works of European and Japanese scientists [21–24] performed under the conditions simulating "microgravity" conditions, as well as the study [25], in which delay times of self-ignition of motor fuels with different cetane numbers were measured, and the recent work [26], in which delay times of self-ignition of *n*-decane and *n*-tetradecane were determined under the conditions of a real diesel engine. The results of these experimental works are used below to compare calculations with experimental data.

In practice, for instance, in liquid fuel sprays and drops suspended in gases, the frequently used approximation of a separate drop can be invalid. In comparatively dense suspensions of drops in gases, heating, vaporization, and self-ignition of a separate drop occur under the influence of other drops. Gas parameters around each separate drop cannot then be considered constant, and gas temperature and composition depend on the distance between particles and the properties of the liquid and gas and change with time. Under these conditions, the problem of drop heating and vaporization and drop self-ignition becomes much more complex. These effects are called collective.

The simulation of vaporization and combustion of drops with the inclusion of collective effects is performed using several approaches: two or several drops [27, 28], a regular sequence of drops [29, 30], a group of chaotically arranged drops [31, 32], or a suspension of drops in a gas [33] are considered. The advantages and disadvantages of these approaches were analyzed in detail in [34–39]. The most thorough description of thermodynamic parameter and velocity fields in the space between drops was obtained by considering two interacting drops or a regular (for instance, linear) sequence of drops [40]. "Group" theories and models of a gas suspension as a rule ignore the nonstationary character of heat- and mass-exchange processes in a drop and in its vicinity and the dependence of these processes on the distance between drops.

The purpose of this work was to create and test a physicochemical model of the self-ignition of drops of liquid hydrocarbons with the inclusion of nonstationary and collective interphase interaction effects. The model was supposed to be used in multidimensional numerical calculations of multiphase reacting flows.

PROBLEM STATEMENT FOR A DROP IN A GAS SUSPENSION

Let us consider a uniform monodisperse suspension of one-species liquid drops in a gas [41, 42]. In such a suspension, all drops have equal sizes and are at equal distances from each other. Equally sized drops uniformly distributed on a plane are schematically shown by solid circles in Fig. 1. Circles around drops characterize the depth of the penetration of diffusion fluxes, that is, conventional boundaries within which the con-

centration of vapor over the liquid and temperature differ from the parameters of the unperturbed gas. The parameters of the unperturbed gas remain stationary as long as circles do not join. When diffusion fluxes from different drops meet, all gas parameters in the space between drops begin to change with time, that is, collective effects come into play.

Because of problem symmetry, we can identify a unit cell (shown by the dashed line in Fig. 1) through the surface of which there are no mass and energy fluxes. The characteristic size of the cell R_c equals half the distance between drops. On a plane, the cell has the form of a regular hexagon, and, in space, it is a regular polyhedron with 20 faces having the form of equilateral triangles with side lengths equal to R_c [41, 42].

It follows that the inclusion of collective effects generally requires solving a nonstationary three-dimensional problem with "external" boundary conditions of zero mass and energy fluxes through the faces of such a unit cell. The volume V_c and surface area S_c of the cell are

$$V_c = \frac{5\sqrt{2}}{3}R_c^3, \quad S_c = 5\sqrt{3}R_c^2.$$

This problem was solved in [41, 42] to show that the flow field in the calculated region was very close to a one-dimensional spherically symmetrical flow field. For this reason, it was suggested in [41, 42] that, instead of the three-dimensional problem, we could solve the spherically symmetrical problem with boundary conditions of zero mass and energy fluxes through the surface of a sphere that modeled the polyhedral unit cell.

In [41, 42], the polyhedral cell was replaced by a spherical unit cell with radius R_e, volume $V_e = (4/3)\pi R^3$, and surface area $S_e = 4\pi R^2$. It follows from the condition of the equality of the sphere and polyhedron volumes ($V_e = V_c$) that the radius of the sphere is

$$R_e = \left(\frac{5\sqrt{2}}{4\pi}\right)^{1/3} R_c \approx 0.826 R_c.$$

The surface areas of the polyhedron and sphere then differ by 1%; that is, $S_e/S_c \approx 0.99$.

A one-dimensional spherically symmetrical problem was formulated in [41–44]. The model was based on nonstationary differential equations of the conservation of mass and energy in the liquid and gaseous phases at variable physical properties. In setting the problem, the concept of multicomponent diffusion in a mixture containing fuel vapor, oxygen, nitrogen, and combustion products was used, and the influence of liquid surface tension forces was taken into account. The model was constructed for a constant pressure in the gas–drop system; that is, $p = p_0 = \text{const}$.

At the initial time $t = 0$, the radius of the unit cell R_c was found from the mass content of the liquid in unit volume of the gas suspension, $\Lambda \ll \rho$, and the initial drop radius R_0,

$$R_c \approx \left(\frac{4\pi}{5\sqrt{2}}\right)^{1/3} R_0(\rho/\Lambda)^{1/3} \approx 1.211 R_0(\rho/\Lambda)^{1/3} \quad (1)$$

or from the equivalence ratio $\Phi = \Lambda/\phi_{st}\rho_g$,

$$R_c \approx \left(\frac{4\pi}{5\sqrt{2}}\right)^{1/3} R_0(\rho/\rho_g\Phi\phi_{st})^{1/3} \approx 1.211 R_0(\rho/\rho_g\Phi\phi_{st})^{1/3}, \quad (2)$$

where ϕ_{st} is the stoichiometric ratio between the fuel and air. The radius of a spherical unit cell is given by

$$R_e \approx R_0(\rho/\Lambda)^{1/3}, \quad (3)$$

$$R_e \approx R_0(\rho/\rho_g\Phi\phi_{st})^{1/3} \quad (4)$$

instead of (1) and (2). Under normal conditions, stoichiometric air–hydrocarbon fuel mixtures are characterized by $\rho_g = 1.19$ kg/m^3, $\rho = 700$–800 kg/m^3, $\phi_{st} \approx 0.06$, and $\Phi = 1$. It follows that, in such mixtures, $\Lambda = \Lambda_{st} \approx 0.07$–$0.08$ kg/m^3, $R_c/R_0 \approx 25$–27, and $R_{e,st}/R_0 \approx 21$–22, where $R_{e,st}$ is the radius of the spherical unit cell in the stoichiometric fuel–air mixture. At elevated pressures, for instance, at the end of the compression cycle in a diesel engine ($\rho_g \approx 30$ kg/m^3), $R_c/R_0 \approx 9$ and $R_e/R_0 \approx 8$.

Since the problem presupposes that pressure is constant, $p = \text{const}$, the parameter R_e (and R_c) depends on time; that is, $R_e = R_e(t)$. The current $R_e(t)$ value is determined in the course of problem solution, and the boundary of the unit cell is allowed to move at a mean gas velocity at point $r = R_e$. Conditions at the boundary of the unit cell therefore have the form

$$r = R_e(t): \frac{\partial T_g}{\partial r} = 0, \quad \frac{\partial G_j y_j}{\partial r} = 0, \quad j = 1, 2, \ldots, M, \quad (5)$$

that is, energy and mass fluxes stop at a finite distance from the drop $r = R_e$ rather than at $r \longrightarrow \infty$. In (5), G_j is the molecular mass of the jth mixture species.

The initial conditions ($t = 0$) have the form

$$R(0) = R_0,$$

$$r < R_0, \quad T(r, 0) = T^0;$$

$$r > R_0, \quad T_m(r, 0) = T_m^0;$$

$$r > R_0, \quad y_j(r, 0) = y_j^0, \quad j = 1, 2, \ldots, M.$$

The problem was solved numerically using the finite-difference method and the method of successive approximations described in detail in [41–44].

THE SELF-IGNITION OF DROPS IN A GAS SUSPENSION

If a drop of a fuel is placed into a heated oxidizing gas (as when a fuel spray is introduced into the combus-

Table 1. Mechanism of self-ignition

Reaction number	Reaction
1	$C_nH_m + (0.5n + 0.25m)O_2 \longrightarrow nCO + 0.5mH_2O$
2	$H_2 + H_2 + O_2 \longrightarrow 2H_2O$
3	$CO + CO + O_2 \longrightarrow CO_2 + CO_2$
4, –4	$CO + H_2O \longleftrightarrow CO_2 + H_2$

Table 2. Kinetic parameters of low-temperature self-ignition of *n*-alkanes

Reaction number	A_{ij}, l, mol, s	m_{ij}	E_{ij}, kcal/mol	Note
1	3.5×10^{13}	0	36.7	*n*-decane
1	1.75×10^{14}	0	36.7	*n*-tetradecane
2	7.0×10^{13}	–0.5	21.0	
3	8.5×10^{12}	–1.5	21.0	
4	1.0×10^{12}	–1.0	41.5	
–4	3.1×10^{13}	–1.0	49.1	

tion chamber of a diesel engine), it can experience self-ignition in some time called self-ignition delay, t_{ign}. According to the Semenov–Frank–Kamenetskii theory [1, 2], self-ignition occurs where the rate of energy release caused by chemical transformations exceeds the rate of heat removal. Self-ignition delay t_{ign} is usually defined as the time during which the maximum rate of temperature increase reaches some preset value, for instance, $T'_{max} = 10^6$ or 10^7 K/s. As a rule, such definitions lead to fairly close t_{ign} values.

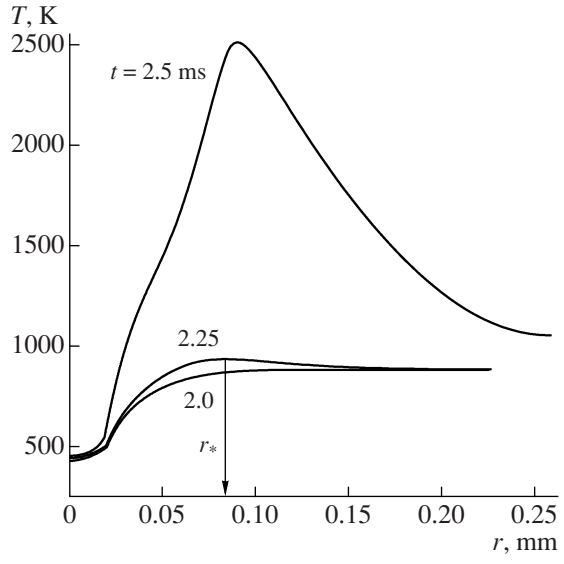

Fig. 2. Calculated spatial distributions of temperature in the self-ignition of an *n*-decane drop in air. Initial parameters: $D_0 = 40$ μm, $T_0 = 300$ K, $T_{g0} = 900$ K, $p = 2$ MPa, and $\Phi = 1.0$.

Detailed kinetic mechanisms are extensively used to study self-ignition and combustion of gaseous hydrocarbons. As concerns drops and sprays of liquid hydrocarbons, detailed kinetic mechanisms are used very rarely to study their self-ignition and combustion [18, 19] because the kinetic mechanisms of the oxidation of the higher hydrocarbons have scarcely been studied and because complex physical processes occur when drops experience self-ignition and combustion. This is the reason why we model self-ignition and combustion of paraffin hydrocarbon drops using an empirical reaction mechanism only including five reactions with the participation of six species (fuel, O_2, CO, CO_2, H_2, and H_2O). This mechanism is presented in Table 1.

The rate of the chemical reactions included in Table 1 was calculated by the equation

$$w_{ij} = K_{ij}P^{mij}\exp(-E_{ij}/RT)\prod_j n_j,$$

where K_{ij} is the preexponential factor and E_{ij} is the activation energy. Note that reaction no. 1 is treated as a bimolecular reaction between the fuel and oxygen. The kinetic parameters of reactions nos. 1, 2, 3, 4, and –4 (back reaction) for *n*-decane and *n*-tetradecane are listed in Table 2.

In [45–47], the self-ignition mechanism similar to that presented in Tables 1 and 2 was verified for the problem of the self-ignition of separate *n*-heptane drops by comparing the calculated and experimental self-ignition delay times. It was found that this mechanism in combination with the model described above fairly well predicted self-ignition delay times for *n*-heptane drops under "microgravity" conditions.

The calculated self-ignition parameters for an *n*-decane drop with the initial diameter 40 μm in a stoichiometric ($\Phi = 1$) suspension of drops in air at the initial liquid temperature $T_0 = 300$ K, air temperature $T_{g\infty} = 900$ K, and pressure $p = 2$ MPa are shown in Figs. 2 and 3. The self-ignition of fuel vapor occurs at some distance r_* from the surface of a drop (Fig. 2).

After self-ignition, the temperature in the vicinity of the $r = r_*$ point rapidly increases with time, and a spherical layer with a finite thickness and a high temperature (up to 2500 K) forms around the drop. In the vicinity of the maximum temperature point (within a flame), the concentrations of fuel vapor and oxygen tend to zero (Fig. 3, time moment $t = 2.5$ ms). After the appearance of a flame around the drop, the mass fraction of vapor on the surface of the particle increases from approximately $y_{vi} = 0.55$ to $y_{vi} = 0.78$.

The calculated self-ignition delay times for *n*-tetradecane drops with the initial diameter 20 μm are compared in Fig. 4 with the self-ignition delay times of motor fuels with different cetane numbers measured in [25] (solid lines) under the conditions close to those in

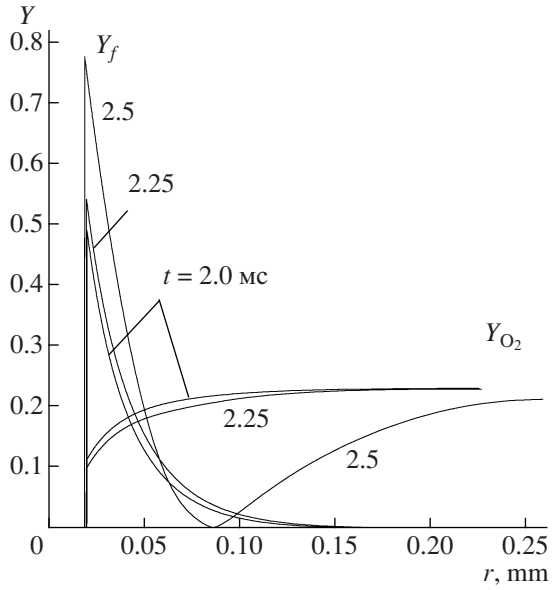

Fig. 3. Calculated spatial distributions of the mass fractions of oxygen and fuel vapor in the self-ignition of an *n*-decane drop in air. Initial parameters: D_0 = 40 μm, T_0 = 300 K, T_{g0} = 900 K, p = 2 MPa, and Φ = 1.0.

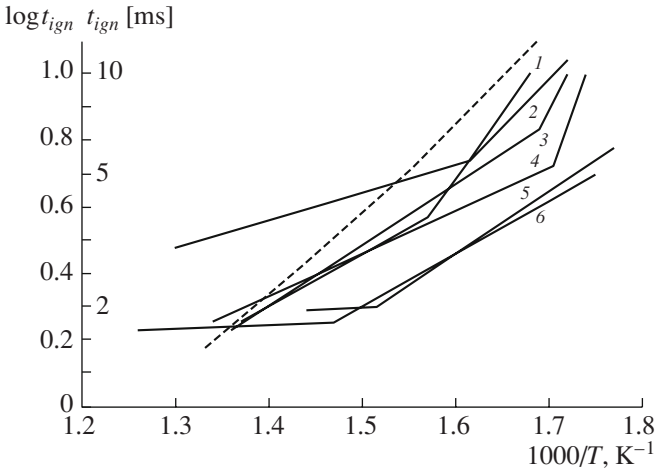

Fig. 4. Comparison of the temperature dependences of the calculated and experimental [25] self-ignition delay times for various fuels at pressure 2.5 MPa. The dashed line corresponds to *n*-tetradecane drops with the initial diameter D_0 = 20 μm. Solid curves correspond to motor fuels with different cetane numbers (CN) and different sprayers (1 and 2). CN/sprayer: (*1*) 49/1, (*2*) 50/1, (*3*) 49/2, (*4*) 50/2, (*5*) 70/2, and (*6*) 62/2.

a diesel engine (pressure p = 2.5 M Pa and air temperature $T_{g\infty}$ = 570–800 K). We see that the model that we use fairly closely agrees with the experimental data [25].

The calculated self-ignition delay times of *n*-decane and *n*-tetradecane drops with various initial diameters are compared in Fig. 5 with self-ignition delay times measured in a real diesel engine [26] (the horizontal line). Calculations were performed for typical conditions in a diesel engine (T_{g0} = 800 K, p = 4 MPa, and Φ = 1.0). It follows from Fig. 5 that the calculated self-ignition delay times are fairly close to their experimental values, especially if it is taken into account that there is drop-size distribution in real sprays, and the real diesel engine fuel is a mixture of hydrocarbons with a mean number of carbon atoms of 13–14. Moreover, self-ignition occurs in a diesel engine at variable pressure and temperature.

THE COMBUSTION OF DROPS SUSPENDED IN A GAS

After the appearance of a high-temperature flame around a drop, the stage of drop combustion begins. Like vaporization, the combustion of a drop depends on the density of the gas suspension and differs from the combustion of a separate drop in an unconfined atmosphere. This is illustrated by Figs. 6 and 7, which correspond to uniform suspensions of drops in a gas enriched in (Fig. 6) and depleted of (Fig. 7) fuel.

The calculated spatial distributions of temperature (Fig. 6a) and mass fractions of fuel (Fig. 6b), oxygen (Fig. 6c), CO_2 (Fig. 6d), and CO (Fig. 6e) at various time moments correspond to the self-ignition and subsequent combustion of a drop of *n*-decane with the initial diameter 100 μm in a uniform suspension of drops

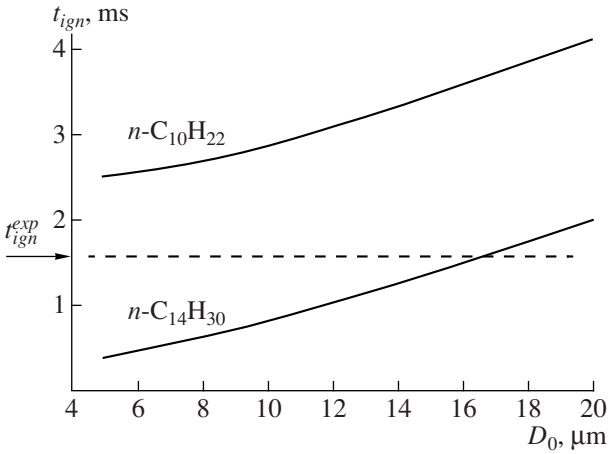

Fig. 5. Comparison of calculated self-ignition delay times with delay times measured in a real diesel engine. Calculations were performed for stoichiometric (Φ = 1.0) gas suspensions of *n*-decane (the upper curve) and *n*-tetradecane (the lower curve) drops with different initial diameters at air temperature and pressure 800 K and 4 MPa, respectively. The horizontal line t_{ign}^{exp} = const corresponds to the experimental diesel engine fuel self-ignition delay time in an engine [26].

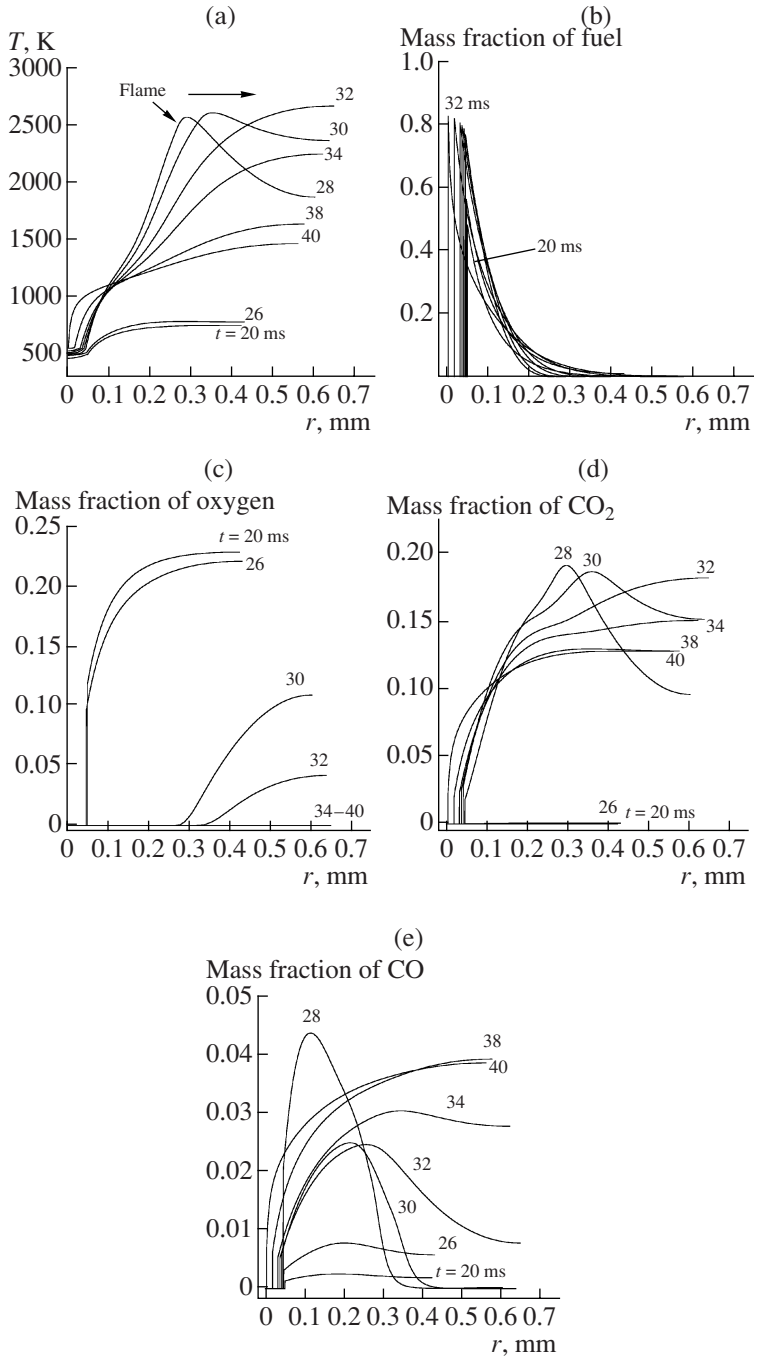

Fig. 6. Calculated spatial distributions of (a) temperature and mass fractions of (b) fuel vapor, (c) oxygen, (d) CO_2, and (e) CO in the self-ignition of an *n*-decane drop with the initial diameter 100 μm in a uniform gas suspension of drops with $\Phi = 2$ at pressure 2 MPa and air temperature 800 K.

in a gas enriched in fuel ($\Phi = 2$) at pressure 2 MPa and air temperature 800 K. It was assumed that, at $t = 0$, drops were instantaneously placed into hot air. Flame appearing after drop self-ignition (approximately at t = 27 ms) then propagates in the direction away from the drop surface at a mean visible velocity of 8–10 cm/s and consumes all the oxygen present in the elementary sphere in time $t \approx 33$ ms. After this, the flame is extinguished, and the drop continues to vaporize. At the moment of combustion cessation, the elementary sphere is filled with unreacted fuel vapor, CO_2, H_2O, H_2, and CO. The understanding of how drops burn in a dense suspension in a gas is very important for the development of simple models of combustion for use in multidimensional gas dynamic calculations.

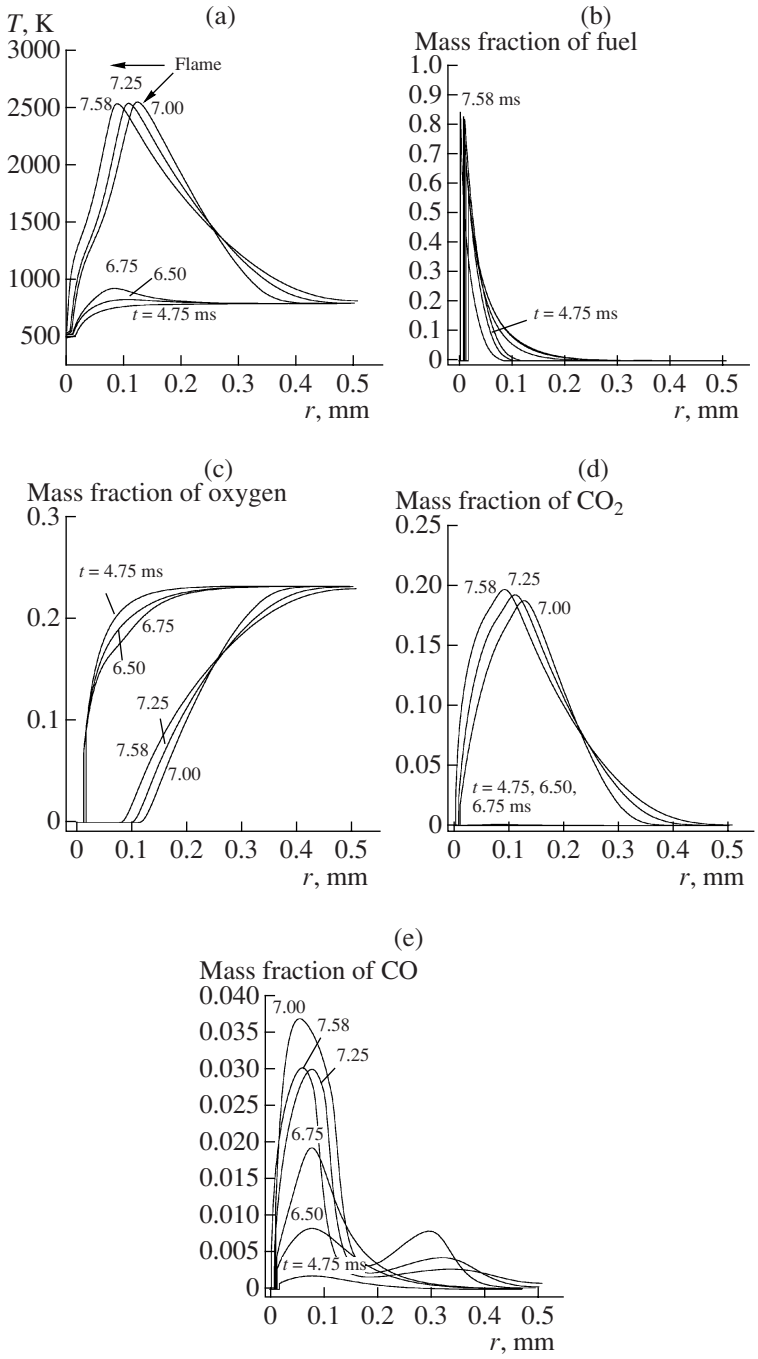

Fig. 7. Calculated spatial distributions of (a) temperature and mass fractions of (b) fuel vapor, (c) oxygen, (d) CO_2, and (e) CO in the self-ignition of an *n*-decane drop with the initial diameter 40 μm in a uniform gas suspension of drops with $\Phi = 0.1$ at pressure 2 MPa and air temperature 800 K.

In Fig. 7, the calculated spatial distributions of temperature (Fig. 7a) and mass fractions of the fuel (Fig. 7b), oxygen (Fig. 7c), CO_2 (Fig. 7d), and CO (Fig. 7e) are shown. The distributions relate to the self-ignition and subsequent combustion of a drop of *n*-decane with the initial diameter 40 μm in a uniform suspension of drops in a gas depleted of the fuel ($\Phi = 0.1$) at pressure 2 MPa and air temperature 800 K. Flame that appears after drop self-ignition (approximately at $t = 6.75$ ms) then propagates in the direction of the drop surface ("collapses") at a visible velocity of about 6 cm/s and consumes almost all the fuel vaporized in the elementary sphere up to $t \approx 7.6$ ms. The combustion of a drop in a gas suspension strongly depleted of fuel resembles the combustion of a separate drop in unconfined atmosphere.

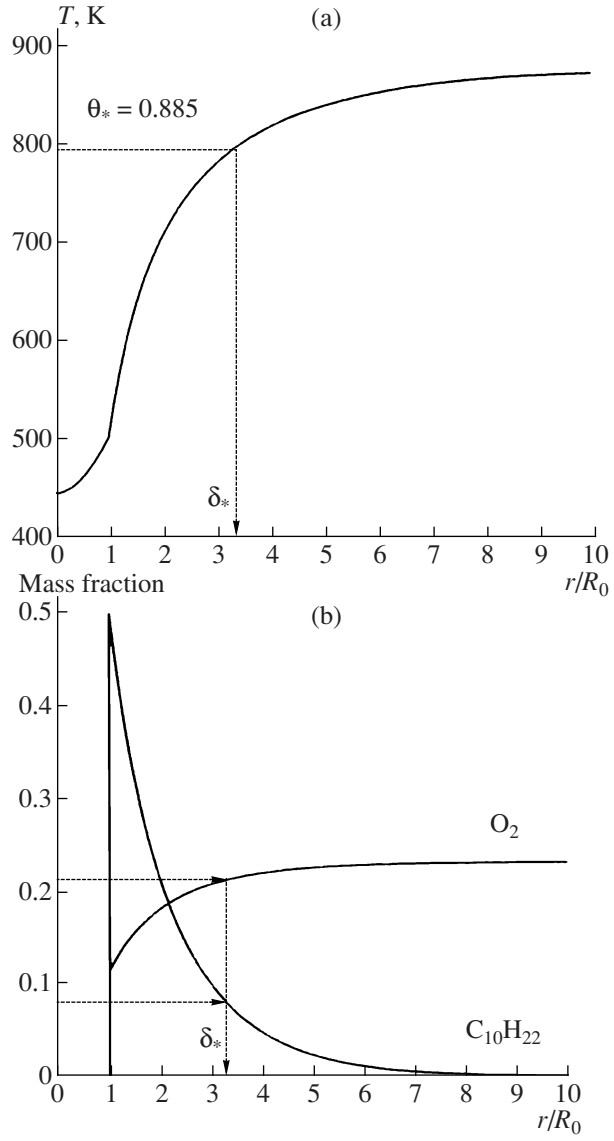

Fig. 8. Determination of (a) reduced temperature and (b) local equivalence ratio in a vapor-gas mixture at the reduced self-ignition radius.

CORRELATION BETWEEN THE VAPORIZATION AND SELF-IGNITION OF DROPS IN GAS SUSPENSION

The complete model of vaporization, self-ignition, and combustion of drops described above was used to perform two series of calculations: (1) calculations of the self-ignition and combustion of drops and (2) calculations of the vaporization of drops (with zero chemical sources in the equations for the energy of the gas phase and diffusion of gas mixture species). Some 200 calculations were performed over wide ranges of the initial diameters of drops (D_0 = 20–150 μm), gas suspension equivalence ratios (Φ = 0.1–2.0), pressures (p = 2–8 MPa), and air temperatures (T_{g0} = 800–900 K) for two hydrocarbons, *n*-decane and *n*-tetradecane. It was assumed that the characteristics obtained for these hydrocarbons could be used to model the ignition of diesel engine fuels.

In calculations of the self-ignition of drops, we intentionally concentrated on the spatial temperature distribution in the vicinity of the particle (1) immediately before self-ignition, (2) at the instant of self-ignition, and (3) immediately after the completion of local self-ignition with the formation of a flame, as is shown in Fig. 2. In Fig. 2, the first time moment is t = 2.0 ms, the second one is t = 2.25 ms, and the third time moment is t = 2.5 ms.

This approach was used to determine self-ignition delay times t_{ign} (approximately 2.25 ms in Fig. 2) and the place of self-ignition determined by the distance r_* from the center of the drop ($r_* \approx 0.085$ mm in Fig. 2). To generalize the data obtained, we introduced the concept of the reduced self-ignition radius $\delta_* = 2r_*/D_0$ ($\delta_* \approx 4.25$ in Fig. 2). The most important result of our calculations was the conclusion that the reduced self-ignition radius weakly depended on the determining parameters of the problem, namely, surrounding air temperature, pressure, equivalence ratio in the gas suspension of drops, the initial diameter of drops, and the type of the fuel. We found that

$$\delta_* = \frac{2r_*}{D_0} = 2.0\text{–}6.5.$$

To summarize, self-ignition delay calculations allowed us to create a database of self-ignition delay times t_{ign} for *n*-decane and *n*-tetradecane drops under various conditions and of reduced self-ignition radii δ_*.

The main purpose of calculations of the vaporization of drops was to determine the local equivalence ratio in a vapor-gas mixture ϕ (it differs from the equivalence ratio in gas suspension Φ) and reduced temperature $\theta_* = (T/T_{g0})_*$ at the reduced self-ignition radius δ_* obtained from drop self-ignition calculations. In other words, we were interested in the $\phi_* = \phi(\delta_*)$ and $\theta_* = (T/T_{g0})_* = T(r_*)/T_{g0}$ values at time $t = t_{ign}$. It is shown in Fig. 8 how the θ_* and δ_* values were determined.

Fig. 9 illustrates the procedure for the determination of θ_* and ϕ_* for the example of t_{ign} = 9.25 ms and δ_* = 4.6. The curves in Fig. 9 were constructed using the results of drop vaporization calculations and represent "trajectories" of points with constant reduced temperatures θ_* = 0.885 and 0.8975 and points with constant ϕ_* = 1.63 in space–time coordinates. We see that curves with θ_* = 0.885 and ϕ_* = 1.63 pass through the point t_{ign} = 9.25 ms, δ_* = 4.6). In other words, local self-ignition in the vicinity of a drop occurs at θ_* = 0.885 and ϕ_* = 1.63. As expected, the results are fairly sensitive to the reduced temperature value. The data presented in Fig. 9 can be interpreted as follows: the local self-ignition of a drop occurs when the reduced temperature and equivalence ratio of the vapor–gas mixture at distance δ_* reach the values θ_* = 0.885 and ϕ_* = 1.63. Indeed,

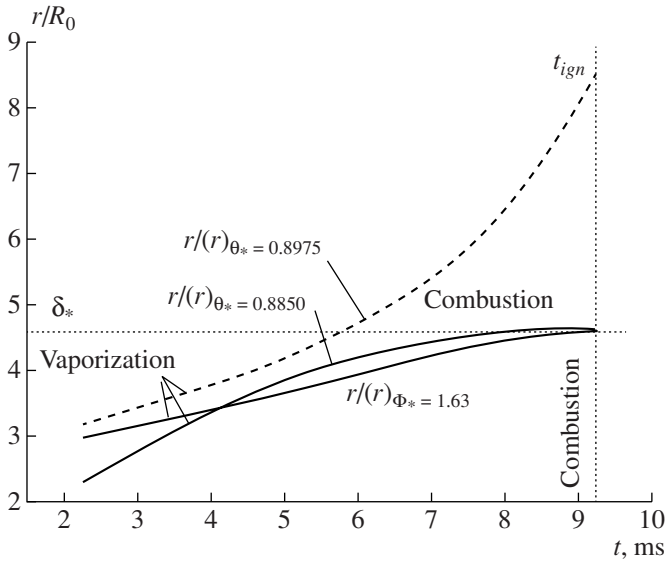

Fig. 9. Determination of the criterion of drop self-ignition.

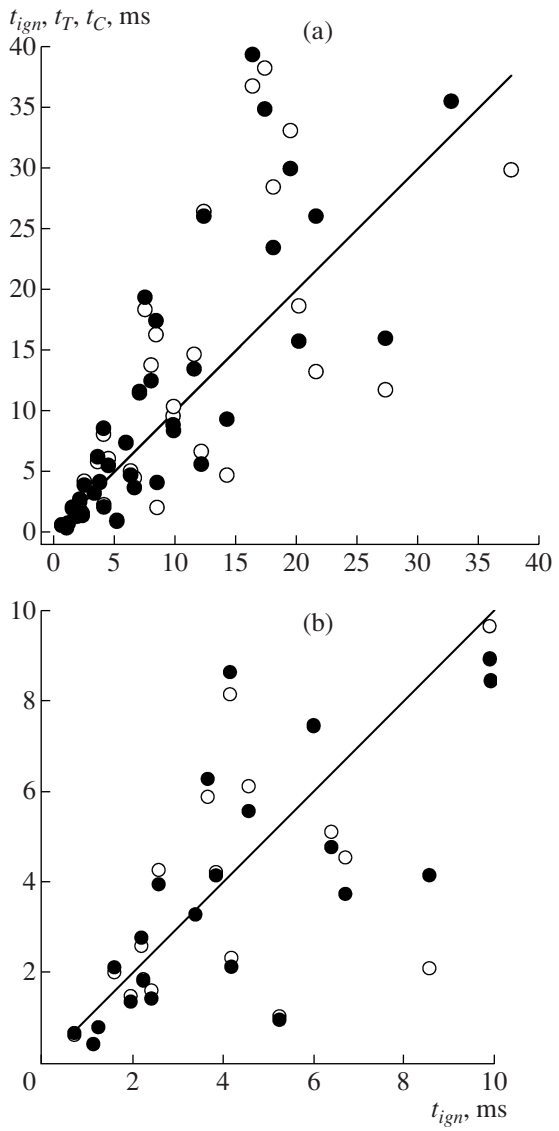

Fig. 10. Correlations between delay times t_{ign} (solid lines) calculated using the model of the self-ignition of drops and delay times t_T (○) and t_C (●) obtained using the self-ignition criteria $\theta_* = 0.906$ and $\phi_* = 0.625$: (a) results of all calculations and (b) results of calculations with $t_{ign} \le 10$ ms.

these θ_* and ϕ_* values are reached at the reduced distance δ_* at $t = t_{ign}$.

A similar comparative analysis was performed for the whole series of calculations. We found that θ_* changed from 0.83 to 1.0, and ϕ_*, from 0.25 to 2.0. A statistical analysis of the data revealed important correlations between drop vaporization and self-ignition calculations. The correlations of the calculated t_{ign} values with t_T (self-ignition delay obtained using the θ_* = const criterion from drop vaporization calculations) and t_C (self-ignition delay obtained on the basis of the ϕ_* = const criterion from drop vaporization calculations) are shown in Figs. 10a and 10b. In Fig. 10a, all the calculation data were used, and, in Fig. 10b, only calculations in which t_{ign} did not exceed 10 ms (important for applications to the working cycle in a diesel engine). The best agreement (the smallest root-mean-square deviation) between t_{ign} and t_T on the one hand and between t_{ign} and t_C on the other was attained at

$$\delta_* = 3.71, \quad \theta_* = 0.91, \quad \phi_* = 0.63. \qquad (6)$$

The conclusion can be drawn that the data presented in Fig. 10 are evidence of the existence of approximate correlation between the t_{ign}, t_T, and t_C values. Importantly, this correlation is universal and independent of the type of the fuel (*n*-decane or *n*-tetradecane), the initial diameter of drops (from 5 to 150 μm), equivalence ratio in a gas suspension of drops (from 0.1 to 2.0), the initial air temperature (from 800 to 900 K), and pressure (from 2 to 8 MPa).

Conditions (6) can be used as a criterion of drop self-ignition (self-ignition criterion in what follows). Maximum root-mean-square deviations from equations (6) are of 70% for the reduced temperature θ_* and 100% for the equivalence ratio ϕ_*, which can be considered quite satisfactory for such a phenomenon as self-ignition. Recall that errors of 100% in kinetic calculations are as a rule considered acceptable because of errors in self-ignition delay measurements and uncertainties in kinetic constants.

The calculated dependences of self-ignition delay times t_{ign}, t_T, and t_C on the initial diameter of drops are shown in Fig. 11. The t_{ign} value decreases and tends to the self-ignition delay of a homogeneous mixture (shown by the horizontal dashed line in Fig. 11) rather than zero as the initial diameter of drops diminishes. Note that, as distinct from the self-ignition of a drop, the summed rate of chemical transformations in a homogeneous mixture is independent of diffusion pro-

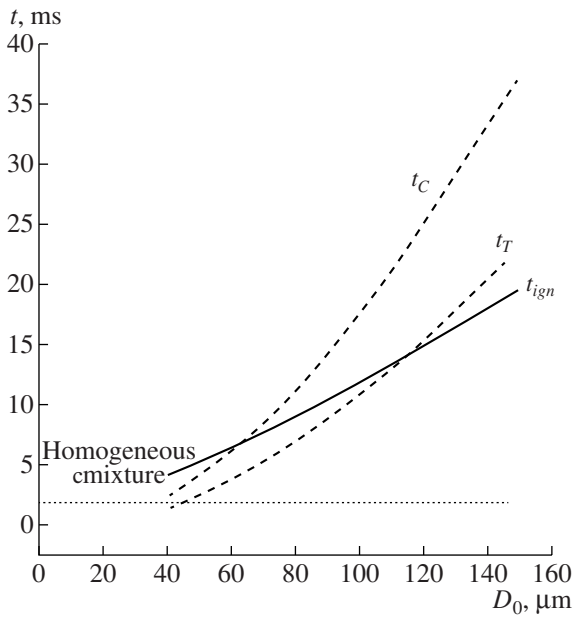

Fig. 11. Calculated dependences of self-ignition delay times t_{ign}, t_T, and t_C on the initial diameter of *n*-decane drops at T_{g0} = 850 K and p = 2 MPa.

cesses. As concerns the behavior of the curves for t_T and t_C in Fig. 11, these values lessen and tend to zero as the diameter of a drop decreases. This shortcoming of self-ignition criteria (6) is easy to remove. Merely, it must be borne in mind that there is a limiting minimum self-ignition delay in the ignition of drops, that is,

$$t_T \geq t_{ign,\,h}, \quad t_C \geq t_{ign,\,h},$$

where $t_{ign,\,h}$ is the self-ignition delay of a homogeneous mixture under equal conditions. In practice, under diesel engine conditions, we always have

$$t_{ign} \geq 0.7\text{–}1.0 \text{ ms}.$$

This condition is related not only to a finite rate of chemical transformations and diffusion deceleration of reactions but also to a finite time of the disintegration of a fuel spray.

The calculated self-ignition delay times $t_{ign,\,h}$ for a homogeneous stoichiometric mixture of *n*-decane and air obtained using a detailed kinetic mechanism [48] are listed in Table 3. These delays correspond to the region of two-stage low-temperature self-ignition of *n*-decane, where the temperature coefficient of the reaction rate is negative. At T < 800 K and p < 2 MPa, self-ignition delay time rapidly increases and can even exceed the drop lifetime for drops with the largest initial diameter used in calculations. The data presented in Table 3 can be used to estimate the limiting minimum t_{ign} values at various pressures and air temperatures.

Table 3. Self-ignition delay times (ms) for an *n*-decane–air homogeneous stoichiometric mixture

T, K	p = 2 MPa	p = 4 MPa	p = 6 MPa	p = 8 MPa
700	12.0	9.69	8.65	7.97
750	3.61	2.58	2.15	1.98
800	2.09	1.24	0.933	0.768
850	2.15	1.06	0.723	0.549
900	2.63	1.20	0.767	0.555
950	3.46	1.47	0.893	0.629

A NEW MODEL OF THE SELF-IGNITION AND COMBUSTION OF DROPS IN A GAS SUSPENSION

A new model of the self-ignition of drops is based on our model of the vaporization of drops [49, 50] augmented by local spatial distributions of temperature and fuel vapor concentration in the vicinity of drops.

The main idea in the extension of model [49, 50] is to redistribute the temperature of the vapor–gas mixture and the concentration of fuel vapor in the grid cell where a drop is situated. The redistribution should preserve the corresponding mean values of temperature $T_{g\infty}$ and fuel vapor concentration $y_{v\infty}$ on the one hand and, on the other, provide a more accurate description of the spatial distribution of the corresponding mixture parameters in the vicinity of a drop, $T_g(r, t)$ and $y_v(r, t)$. Given the $T_g(r, t)$ and $y_v(r, t)$ distributions, we can determine the drop self-ignition delay time from changes in the reduced temperature θ_* and equivalence ratio ϕ_* at a distance equal to the reduced radius δ_*: self-ignition occurs if criteria (6) are fulfilled.

Let R_d be the depth of heat wave penetration from the surface of a drop into gas surrounding it. An analysis of detailed calculations of drop vaporization (see Figs. 7, 8) shows that the temperature profile in the vicinity of a drop can be approximated by a parabola at $R \leq r \leq R_d$,

$$T_g(r) = T_i + a(r - R) + b(r - R)^2, \tag{7}$$

and by the equation

$$T_g(r) = T_d,$$

at $R_d \leq r \leq R_e$. Here, T_i is the temperature of the surface of the drop and $T_d = T_g(R_d)$. At the distance $r = R_d$, the derivative of temperature with respect to radius is zero. Therefore,

$$a = -2b(R_d - R). \tag{8}$$

It follows from the condition $T_d = T_g(R_d)$ that

$$b = -\frac{T_d - T_i}{(R_d - R)^2}. \tag{9}$$

Substituting (8) and (9) into (7) yields the temperature profile in the vicinity of a vaporizing drop within an equivalent sphere with radius R_e,

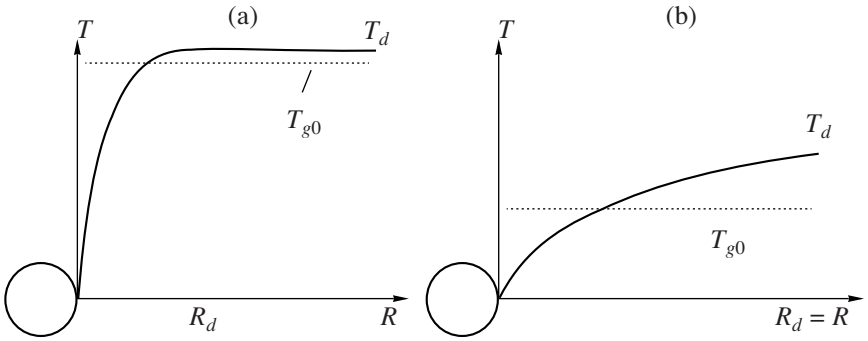

Fig. 12. Scheme of temperature profiles in the vicinity of a drop at (a) $t < t_d$ and (b) $t > t_d$.

$$T_g(r) = T_i + 2(T_d - T_i)\frac{r-R}{R_d-R} - (T_d - T_i)\left(\frac{r-R}{R_d-R}\right)^2 \quad (10)$$

$$\text{at} \quad R \le r \le R_d,$$

$$T_d = T_g(R_d) \quad \text{at} \quad R_d \le r \le R_e.$$

To summarize, the temperature is constant (maximum, T_d) at $R_d \le r \le R_e$ (Fig. 12). It follows that the heat flux to the surface of a drop is determined by the T_d temperature rather than the mean gas temperature in the grid cell (T_{g0}). However, the replacement of T_d with T_{g0} should not influence the heat balance in the grid cell; that is, the mean temperature in the cell, T_{g0}, should remain unchanged. If, as a first approximation, the temperature dependence of heat capacity is ignored, the mean temperature in the grid cell should equal the mean integral temperature in the elementary sphere.

When thermal perturbation reaches the boundary of the elementary sphere around a drop, the gas temperature in the space between neighboring drops ceases to be constant. It follows that we can determine the time interval t_d during which T_d = const. At $t > t_d$, the T_d temperature equals the temperature at the boundary of the elementary sphere.

The model described above includes two independent values: the temperature T_d and the radius R_d. R_d can be determined from the condition that the temperature reaches a maximum at $r = R_d$. In addition, the unknown values T_d and R_d are related by the heat balance equation. The spatial distribution of the mass fraction of fuel vapor is modeled similarly. The moment of drop self-ignition corresponds to the moment at which criteria (6) are satisfied; that is, each drop has its own self-ignition delay time t_{ign} determined by these criteria in a gas suspension.

After ignition, a drop begins to burn. It can therefore be assumed that, at $t = t_{ign}$, the heat flux toward the surface of the drop changes stepwise from the heat flux determined by the difference of temperatures $T_d - T_i$ to the heat flux determined by the difference $T_b - T_i$, where T_b is the combustion temperature. As concerns the mass flux of vapor from the surface of the drop, it changes abruptly from the value determined by the difference of mass fractions $y_{vs} - y_{v\infty}$ to the value determined by the concentration of vapor on the surface of the drop, y_{vi}, because $y_{v\infty} \longrightarrow 0$ in the flame front. The combustion temperature is determined by the equation

$$T_b = T_d + \frac{y_{ox,\infty} Q_{ox}}{c_p} \quad \text{at} \quad y_{ox,\infty} < y_{ox,st},$$

$$T_b = T_d + \frac{y_{ox,st} Q_{ox}}{c_p} \quad \text{at} \quad y_{ox,\infty} \ge y_{ox,st},$$

where $y_{ox,\infty}$ is the mass fraction of the oxidizer in the space on the outside of the flame, $y_{ox,st}$ is the stoichiometric mass fraction of the oxidizer, Q_{ox} is the heat of the reaction per unit mass of the oxidizer, and c_p is the heat capacity of the mixture at some reference temperature. Note that, in terms of this model, the diffusion combustion of a drop reduces to the instantaneous transformation of all fuel vaporized during a time step into combustion products and the release of the corresponding reaction heat.

During time t_{ign}, drops vaporize, and a homogeneous spatially nonuniform vapor–air mixture is formed around them. Therefore, at times exceeding t_{ign}, we must take into account not only the possibility of formation of a diffusion flame around drops, but also the possibility of homogeneous combustion of vaporized fuel in the gas phase. There are several simple models of homogeneous turbulent combustion, for instance, the well-known model of eddy breakup [51].

CALCULATION RESULTS

We performed two series of multidimensional numerical calculations to verify the new model of self-ignition and combustion of drops.

In the first series, we used a uniform square computational grid. One of the grid cells contained 27 drops of *n*-decane uniformly distributed in its volume. It was assumed that, at the initial time, gas (air) and drops were at rest. The equivalence ratio Φ in the cell with drops was varied by varying the size of drops.

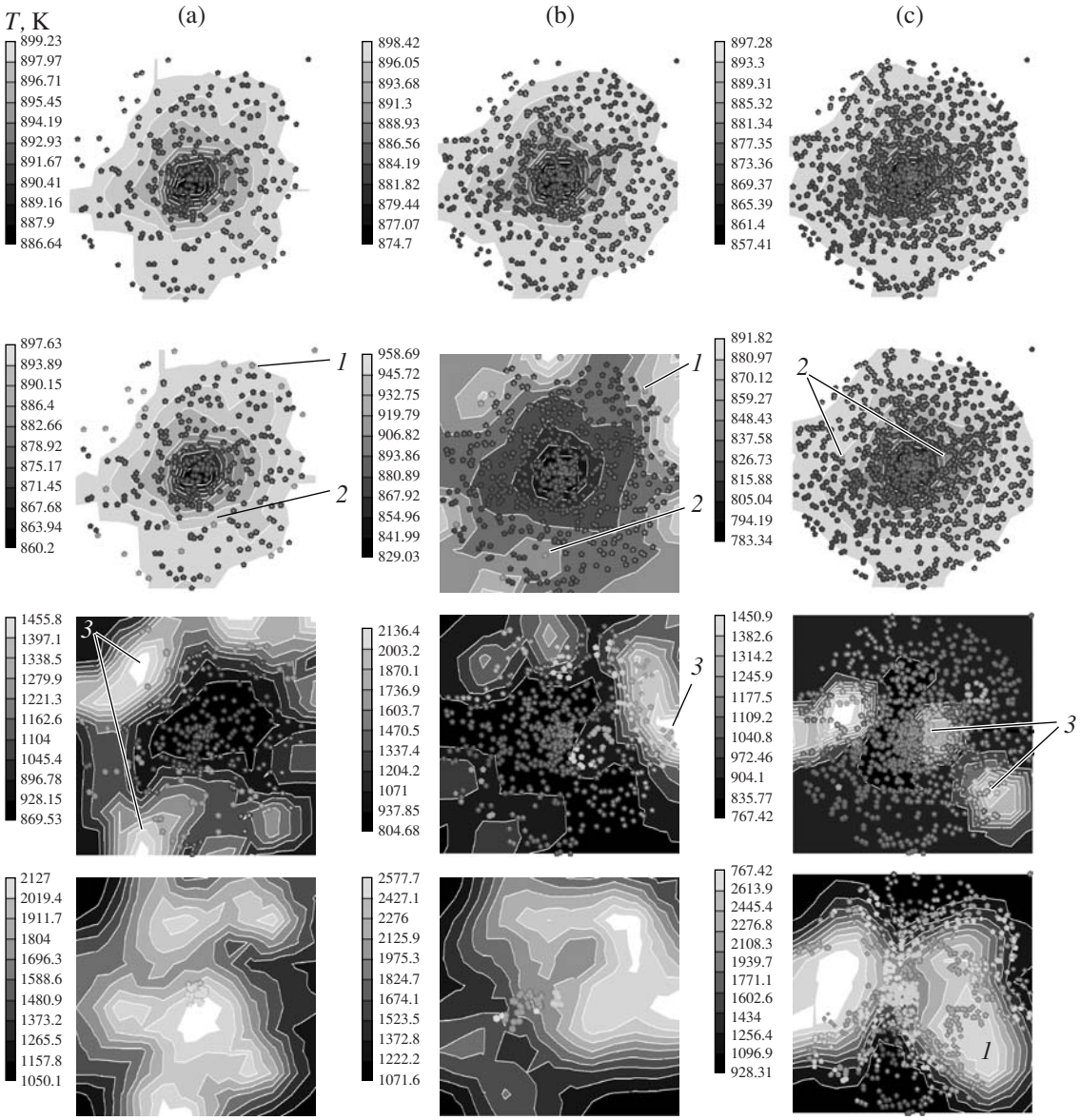

Fig. 13. Calculated gas temperature fields (scale and isolevels) for the self-ignition and combustion of a nonuniform monodisperse cloud of *n*-decane drops at 1, 3, 6, and 9 ms (from top to bottom). Drop diameter $d = 60$ μm, initial gas temperature $T_0 = 900$ K, pressure $p = 2$ MPa, number of drops in a cloud: (a) 300, (b) 600, and (c) 900. Arrows: (*1*) self-ignition of drops at the periphery of clouds, (*2*) self-ignition of drops in the region with a low number density of particles, and (*3*) regions of homogeneous combustion.

The results of calculations were analyzed to determine the criterion of self-ignition in the δ_* and θ_* variables, similarly to what was done to obtain criteria (6). As in (6), it was assumed that $\theta_* = 0.91$. We found that, for the simplified new model, the criterion of self-ignition with respect to reduced temperature had the form

$$\delta_* = 5.0, \quad \theta_* = 0.91. \qquad (11)$$

It follows that, as distinct from criterion (6), drop self-ignition occurs in the simplified model when reduced temperature $\theta_* = 0.91$ is reached at reduced distance $\delta_* = 5.0$ (instead of 3.71). If (11) is satisfied, the results of calculations according to the simplified model very closely agree with the detailed calculation data.

The results of three-dimensional calculations of self-ignition and combustion of nonuniform clouds of (a) 300, (b) 600, and (c) 900 identical *n*-decane drops ($D_0 = 60$ μm) in 1 cm^3 of air at the initial gas temperature $T_{g0} = 900$ K and pressure $p_0 = 2$ MPa are shown in Fig. 13. The number density of the distribution of drops over the volume decreases as the distance from the center of the cloud increases. We used a simple structured computational grid. The problem was solved taking into account gas and particle motions; that is, complete (Reynolds-averaged) Navier–Stokes equations, equa-

tions of the conservation of energy for the gas phase (with sources describing interphase mass, momentum, and energy exchange), and equations of the conservation of mass, momentum, and energy for each drop (with the use of the Lagrange formalism) were solved. The turbulence of the gas phase was described by the well-known $k - \varepsilon$ model, and turbulent dispersion of drops, by the model suggested in [52]. The calculations were performed using the AVL FIRE V8.6 commercial package with introduced user functions.

Immediately after the self-ignition of some drop, its diffusion burning according to the model described above began. In addition to diffusion burning, we also took into account homogeneous burning of fuel vapor, the rate of which was described by the model from [51]. Variants a, b, and c shown in Fig. 13 were used to simulate the behavior of fuel–air mixtures strongly depleted of fuel on average, but with substantially different local number densities of drops.

The brightness background in Fig. 13 corresponds to gas temperature in the space between drops. A darker background corresponds to a colder gas. Drop vaporization causes gas cooling, and this effect is more pronounced in the denser central part of the cloud.

The first self-ignition event occurs in places where collective effects are insignificant, at the periphery of the cloud (arrows *1* in Figs. 13a, 13b) or in rarefied local cloud regions (arrows *2* in Figs. 13a–13c). Ignition delay (time before the first self-ignition event in the cloud) was the same in all cases, although the numbers of ignited drops were substantially different (27 drops in Fig. 13a, 13 drops in Fig. 13b, and only two drops in Fig. 13c). Subsequent self-ignition events either were independent of the preceding ones or occurred as a result of a flow of a hot mixture of air with combustion products past vaporizing drops. In some cloud regions, homogeneous combustion of fuel vapor was observed; it was caused by the appearance of combustion products from ignited drops (arrows *3* in Figs. 13a–13c). With time, burning spots propagated to layers with larger number densities of drops. Only at the end of the process, drops in the central part of the cloud with a maximum number density of drops experienced ignition.

The sequence of frames in Figs. 13a and 13b is evidence that a cloud burns from periphery to its center. In the last frames, we only see central drops, whereas all the peripheral drops have either vaporized or been burnt in diffusion flames. Anisotropy of cloud burning out is shown in Fig. 13c.

On the whole, the combustion of a cloud of drops with a more dense core (Fig. 13c) differs substantially from the combustion of drop clouds with smaller core densities (Figs. 13a, 13b). The process in Fig. 13c is characterized by a much lower intensity and uniformity of cloud burning out.

CONCLUSIONS

A parametric analysis of numerical solutions to the problems of the vaporization and self-ignition of drops according to the complete model allowed us to suggest a new criterion of drop self-ignition. According to this criterion, ignition occurs when, at a given reduced distance from the surface of a drop, a definite reduced gas temperature and a definite equivalence ratio are reached.

A new model of drop heating and vaporization was suggested for use in multidimensional gas dynamic calculations. The central idea of the model is the redistribution of vapor-gas mixture temperature and fuel vapor concentration in the grid cell containing a drop. The redistribution should preserve the corresponding mean gas temperature and fuel vapor concentration (gas dynamic equations are solved for mean parameters) on the one hand and more accurately describe the spatial distribution of mixture parameters around a drop on the other. The distribution of gas temperature and liquid vapor concentration around a drop and the new self-ignition criterion can be used to determine drop self-ignition delay time from changes in reduced temperature and equivalence ratio at the reduced distance from the drop; self-ignition occurs when criteria (6) are satisfied.

The model of drop heating and vaporization and the criterion of self-ignition were used to create a new self-ignition (and combustion) model for liquid hydrocarbon drops in dense gas suspensions. The model was verified by performing multidimensional calculations of the self-ignition and combustion of a cloud of drops. Calculations showed that the model correctly described the phenomenology of the process: the cloud experienced self-ignition and burned from its periphery to the center. The first self-ignition events occurred at the periphery of the cloud, where collective effects were insignificant. Subsequently, combustion sporadically occurred in layers situated closer to the center of the cloud. Only at the end of the process, drops in the central (dense) cloud region experienced self-ignition. It follows that the new model is the first one that allows the phenomenology of the local appearance and anisotropic propagation of self-ignition and combustion waves to be reproduced. Similar characteristics were observed experimentally in the self-ignition of fuel sprays in diesel engines. Self-ignition always occurs in several spots at the periphery of a spray and then propagates along the spray and inside it exhibiting anisotropy and propagation nonuniformity.

ACKNOWLEDGMENTS

This work was financially supported by the Russian Foundation for Basic Research, project nos. 08-08-00068 and 07-08-00558.

REFERENCES

1. N. N. Semenov, *Chain Reactions* (ONTI, Leningrad, 1934), p. 110 [in Russian].
2. D. A. Frank-Kamenetskii, *Diffusion and Heat Transfer in Chemical Kinetics* (Akad. Nauk SSSR, Moscow, 1947) [in Russian].
3. G. A. Varshavskii, *Combustion of Drops of Liquid Fuel* (BNT, Moscow, 1945) [in Russian].
4. J. Lorell, H. Wise, and R. S. J. Carr, J. Chem. Phys. **35**, 2 (1956).
5. F. A. Agafonova, M. A. Gurevich, and I. I. Paleev, Zh. Tekh. Fiz. **27**, 1818 (1957) [Sov. Tech. Phys. **2**, 1689 (1957)].
6. C. E. Polymeropoulos and R. L. Peskin, Combust. Flame **13** (2), 166 (1969).
7. G. A. Varshavskii, D. V. Fedoseev, and D. A. Frank-Kamenetskii, Fiz. Aerozolei, No. 1, 101 (1966).
8. M. A. Gurevich, G. I. Sirkunen, and A. M. Stepanov, Fiz. Aerodispers. Sist., No. 6, 52 (1972).
9. Yu. I. Gol'dshleger and S. D. Amosov, Fiz. Goreniya Vzryva **13** (6), 813 (1977).
10. V. N. Bloshenko, A. G. Merzhanov, N. I. Peregudov, and B. I. Khaikin, in *Proc. of the III All-Union Symp. on Combustion and Explosion* (Inst. Khim. Fiz., Akad. Nauk SSSR, Chernogolovka, 1971), p. 81.
11. V. N. Bloshenko, A. G. Merzhanov, N. I. Peregudov, and B. I. Khaikin, in *Combustion and Explosion* (Inst. Khim. Fiz., Akad. Nauk SSSR, Chernogolovka, 1972), p. 227 [in Russian].
12. G. A. E. Godsave, in *Proc. of the 4th Int. Symp. on Combust* (Williams and Wilkins, Baltimore, MD, 1953), p. 818.
13. D. B. Spalding, in *Proc. of the 4th Int. Symp. on Combust* (Williams and Wilkins, Baltimore, MD, 1953), p. 847.
14. M. Goldsmith and S. S. Penner, Jet Propuls. **24** (4), 245 (1954).
15. C. A. Bergeron and W. L. H. Hallett, Can. J. Chem. Eng. **67**, 142 (1989).
16. S.-C. Rah, A. F. Sarofim, and J. M. Beer, Combust. Sci. Technol. **49**, 169 (1986).
17. J. J. Sangiovanni and A. S. Kesten, in *Proc. of the 16th Int. Symp. on Combust* (Combust. Inst., Pittsburgh, PA, 1977), p. 577.
18. A. Cuoci, M. Mehl, G. Buzzi-Ferraris, et al., Combust. Flame **143**, 211 (2005).
19. V. Ya. Basevich, S. M. Frolov, V. S. Posvyanskii, et al., Khim. Fiz. **24** (5), 89 (2005).
20. S. M. Frolov and V. Ya. Basevich, *Combustion Laws*, Ed. by Yu. V. Polezhaev (Energomash, Moscow, 2006), p. 130 [in Russian].
21. P. Massoli, M. Lazzaro, F. Beretta, and A. D'Alessio, in *Report on Research Activities and Facilities*, Ed. by A. di Lorenzo (Instituto Motori C.N.R., Napoli, 1993), p. 36.
22. A. Atthasit, N. Doue, Y. Biscos, et al., in *Combust. and Atmospheric Pollution,* Ed. by G. D. Roy, S. M. Frolov, and A. M. M. Starik (Torus, Moscow, 2003), p. 214.
23. M. Takei, H. Kobayashi, and T. Niioka, Int. J. Microgravity Res. Appl. Microgravity Sci. Technol. **6** (3), 184 (1993).
24. T. Niioka, H. Kobayashi, and D. Mito, in *Proc. of the IVTAM Symp. on Mechanics and Combust. of Droplet and Sprays* (Tainan, 1994), p. 367.
25. A. S. Sokolik and V. Ya. Basevich, Zh. Fiz. Khim. **28**, 1935 (1954).
26. F. X. Tanner, SAE Techn. Paper Series, 2003-01-1044.
27. E. M. Twardus and T. A. Brzustowski, Archiwum Processov Spalania **8**, 347 (1977).
28. H. A. Dwyer, H. Nirschl, P. Kerschl, and V. Denk, in *Proc. of the 25th Int. Symp. on Combustion* (Combust. Inst., Pittsburg, PA, 1994), p. 389.
29. M. Marberry, A. K. Ray, and K. Leung, Combust. Flame **57**, 237 (1984).
30. J. Cuadros, J. Linares, K. Sivasankaran, et al., Int. J. Heat Mass Transfer **39**, 3949 (1996).
31. H. H. Chiu and T. M. Liu, Combust. Sci. Technol. **17**, 127 (1977).
32. S. M. Correa and M. Sichel, in *Proc. of the 19th Int. Symp. on Combustion* (Combust. Inst., Pittsburg, PA, 1983), p. 300.
33. R. I. Nigmatulin, *Dynamics of Multiphase Mediums* (Nauka, Moscow, 1987), Vol. 1 [in Russian].
34. J. C. Kent, Appl. Sci. Res. Ser. A **28**, 315 (1973).
35. C. K. Law, Prog. Energy Combust. Sci. **8**, 171 (1982).
36. W. A. Sirignano, Prog. Energy Combust. Sci. **9**, 291 (1983).
37. W. D. Bachalo, in *Proc. of the 25th Int. Symp. on Combustion* (Combust. Inst., Pittsburg, PA, 1994), p. 333.
38. C. T. Avedisian, J. Propulsion Power **16**, 628 (2000).
39. F. Mashayek and R. V. R. Pandya, Prog. Energy Combust. Sci. **29**, 329 (2003).
40. J. Warnats, U. Maas, and R. W. Dibble, *Combustion* (Springer, New York, 1996; Fizmatlit, Moscow, 2003).
41. S. M. Frolov, V. Ya. Basevich, V. S. Posvyanskii, and V. A. Smetanyuk, Khim. Fiz. **7**, 49 (2004).
42. S. M. Frolov, V. Ya. Basevich, V. S. Posvyanskii, et al., *Modern Problems of Investigations of Fast Processes and Phenomenons of Catastrophic Character* (Nauka, Moscow, 2007), p. 89 [in Russian].
43. S. M. Frolov, V. S. Posvyanskii, V. Ya. Basevich, et al., Khim. Fiz. **23** (4), 75 (2004).
44. S. M. Frolov, in *Proc. of the Int. Conf. on Combust. and Detonation – Zel'dovich Memorial* (Torus, Moscow, 2004), Paper No. OP-07 (CD).

45. S. M. Frolov, V. Ya. Basevich, and V. S. Posvianskii, in *Application of Detonation to Propulsion*, Ed. by G. D. Roy, S. M. Frolov, and J. M. Shepherd (Torus, Moscow, 2004), p. 110.

46. V. Ya. Basevich, S. M. Frolov, and V. S. Posvyanskii, Khim. Fiz. **24** (7), 58 (2005).

47. S. M. Frolov, V. Ya. Basevich, A. A. Belyaev, et al., *Combust. and Pollution: Environmental Effect*, Ed. by G. D. Roy, S. M. Frolov, and A. M. M. Starik (Torus, Moscow, 2005), p. 117.

48. V. Ya. Basevich and S. M. Frolov, Khim. Fiz. **25** (6), 54 (2006).

49. S. M. Frolov, F. S. Frolov, and B. Basara, *Nonequilibrium Processes. V. 1: Combust. and Detonation*, Ed. by G. D. Roy, S. M. Frolov, and A. M. M. Starik (Torus, Moscow, 2005), p. 179.

50. S. M. Frolov, F. S. Frolov, and B. Basara, J. Rus. Laser Res. **27**, 562 (2006).

51. B. F. Magnussen and B. H. Hjertager, Proc. Combust. Institute **16**, 719 (1976).

52. P. J. O'Rourke, J. Comp. Phys. **83**, 345 (1989).